

Measurement for Detection of Incomplete Partition Type II Anomalies on MR Imaging

 K.L. Reinshagen,  H.D. Curtin,  A.M. Quesnel, and  A.F. Juliano

ABSTRACT

BACKGROUND AND PURPOSE: Incomplete partition type II of the cochlea, commonly coexisting with an enlarged vestibular aqueduct, can be a challenging diagnosis on MR imaging due to the presence of a dysplastic spiral lamina–basilar membrane neural complex, which can resemble the normal interscalar septum. The purpose of this study was to determine a reproducible, quantitative cochlear measurement to assess incomplete partition type II anomalies in patients with enlarged vestibular aqueducts using normal-hearing ears as a control population.

MATERIALS AND METHODS: Retrospective analysis of 27 patients with enlarged vestibular aqueducts (54 ears) and 28 patients (33 ears) with normal audiographic findings who underwent MR imaging was performed. Using reformatted images from a cisternographic 3D MR imaging produced in a plane parallel to the lateral semicircular canal, we measured the distance (distance X) between the osseous spiral lamina-basilar membrane complex of the upper basal turn and the first linear signal void anterior to the basilar membrane.

RESULTS: The means of distance X in patients with normal hearing and prospectively diagnosed incomplete partition type II were, respectively, 0.93 ± 0.075 mm (range, 0.8–1.1 mm) and 1.55 ± 0.25 mm (range, 1–2.1 mm; $P < .001$). Using 3 SDs above the mean of patients with normal hearing (1.2 mm) as a cutoff for normal, we diagnosed 21/27 patients as having abnormal cochleas; 4/21 were diagnosed retrospectively. This finding indicated that almost 20% of patients were underdiagnosed. Interobserver agreement with 1.2 mm as a cutoff between normal and abnormal produced a κ score of 0.715 (good).

CONCLUSIONS: Incomplete partition type II anomalies on MR imaging can be subtle. A reproducible distance X of ≥ 1.2 mm is considered abnormal and may help to prospectively diagnose incomplete partition type II anomalies.

ABBREVIATIONS: DRIVE = driven equilibrium; EVA = enlarged vestibular aqueduct; IP-II = incomplete partition type II

Incomplete partition type II (IP-II, scala communis) is one of many congenital malformations associated with sensorineural hearing loss. IP-II has been characterized as a cochlea with a normal proximal basilar turn and a deficient interscalar septum between the upper turns.^{1,2} In combination with an enlarged vestibular aqueduct (EVA), this anomaly was first described by Carlo Mondini³ and is frequently referred to as the “Mondini” deformity. Correlation among CT, MR imaging, and histopathology in this entity has indicated that a band of low signal on MR imaging extending from the lateral modiolus to the lateral wall of the cochlea (closest to the middle ear) near the upper middle turn corresponds to a band of tissue representing the dysplastic osseous

spiral lamina–basilar membrane neural complex. This dysplastic structure contains neurosensory elements, including the dendritic processes of the spiral ganglion neurons and a dysplastic organ of Corti on top of the basilar membrane of the middle turn.⁴ The dysplastic osseous spiral lamina–basilar membrane neural complex has an MR imaging appearance that can mimic that of the interscalar septum. Thus, the IP-II anomaly may be under-recognized on MR imaging.

The presence of an EVA can sometimes herald an underlying IP-II anomaly. Radiologically, IP-II is most often diagnosed in conjunction with EVA, possibly because of limitations in the radiologic diagnosis of IP-II based on current methods and because the EVA draws the radiologist’s attention to a subtle cochlear anomaly. In a recent study using high-resolution CT and 1.5T MR imaging, 92% (54/59) of ears were found to have IP-II with an EVA and 8% (5/59) of ears had an isolated IP-II anomaly.⁵ In contrast, on histologic examination of human temporal bone specimens, 91% (20/22) of ears with IP-II were found to have no associated EVA, suggesting that isolated IP-II cochlear anomalies may be radiologically underdiagnosed.⁶

Received January 31, 2017; accepted after revision June 1.

From the Departments of Radiology (K.L.R., H.D.C., A.F.J.) and Otolaryngology (A.M.Q.), Massachusetts Eye and Ear, Harvard Medical School, Boston, Massachusetts.

Please address correspondence to Katherine L. Reinshagen, MD, Department of Radiology, Massachusetts Eye and Ear, 243 Charles St, Boston, MA 02114; e-mail: katherine_reinshagen@meei.harvard.edu

<http://dx.doi.org/10.3174/ajnr.A5335>

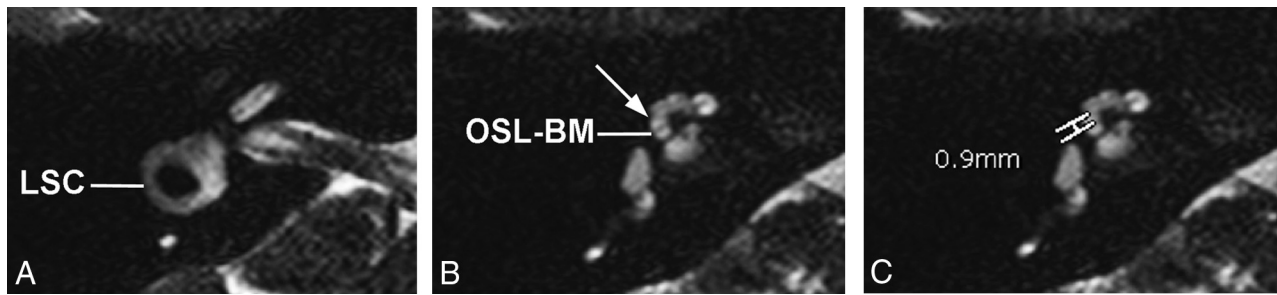


FIG 1. Axial 3D cisternographic (DRIVE) fast-recovery TSE MR imaging of the right temporal bone in a patient with normal hearing. *A*, Reformatted images parallel to the lateral semicircular canal (LSC) are created. Once created, the lateral semicircular canal is seen in its entirety on a single reformatted image. *B*, The osseous spiral lamina–basilar membrane complex of the upper basal turn (OSL-BM) and the first T2-hypointense linear band (*arrow*), in this case representing the interscalar septum, are demonstrated. *C*, A caliper is then placed to measure the distance between the OSL-BM and the linear band (distance X).

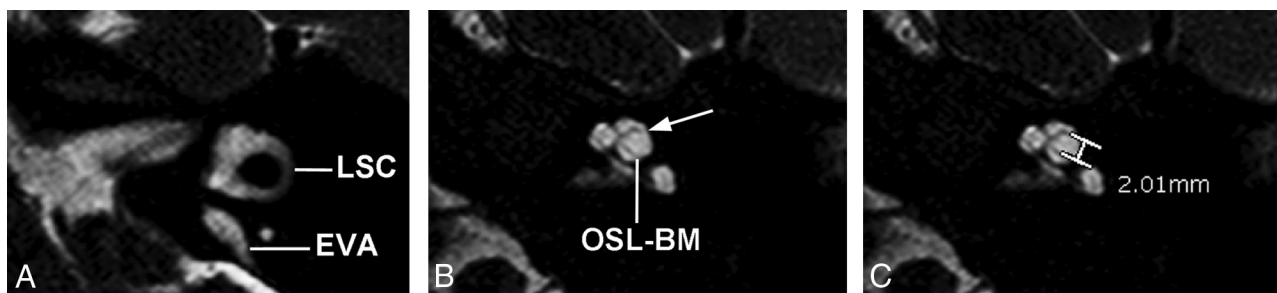


FIG 2. Axial 3D cisternographic (DRIVE) fast-recovery TSE MR image of the right temporal bone in a patient with a prospectively diagnosed IP-II anomaly. *A*, Reformatted images parallel to the lateral semicircular canal (LSC) are created. Once created, the lateral semicircular canal is seen in its entirety on a single reformatted image. Note the enlarged vestibular aqueduct. *B*, The osseous spiral lamina–basilar membrane complex of the upper basal turn (OSL-BM) and the first T2-hypointense linear band (*arrow*), in this case representing a band of dysplastic osseous spiral lamina–basilar membrane neural complex, are demonstrated. *C*, A caliper is then placed to measure the distance between the OSL-BM and the linear band (distance X).

Because the morphologic diagnosis of IP-II can be challenging on MR imaging, our study aimed to determine a quantitative, reproducible measurement technique on MR imaging that would aid in the diagnosis of IP-II. A secondary aim of the study was to determine the prevalence of prospectively underdiagnosed cases of IP-II in patients with enlarged vestibular aqueducts. We hypothesized that because of the partial absence of the interscalar septum in IP-II, the measured distance X would be larger in IP-II than in normal-hearing ears and, when used retrospectively, would help identify missed cases of IP-II.

MATERIALS AND METHODS

Following institutional review board approval, we conducted a retrospective analysis of high-resolution 1.5 and 3T MR imaging temporal bone studies performed between 2005 and 2015 at the Massachusetts Eye and Ear. Patients who underwent a high-resolution 3D heavily T2-weighted cisternographic sequence (axial T2 3D driven equilibrium [DRIVE], Philips Healthcare, Best, the Netherlands; axial CISS, Siemens, Erlangen, Germany) and had a radiologic diagnosis of an enlarged vestibular aqueduct were selected. A separate, consecutively chosen, control group with normal audiographic findings, discussed in the following paragraph, was included in the study. The imaging acquisition parameters for the 3T T2-DRIVE were set as follows: TR, 1700 ms; TE, 190 ms; NEX, 3; spacing, 0.5 mm; matrix, 412 × 337; scan time, 4 minutes 37 seconds. The imaging acquisition parameters for the CISS sequence were set as follows: TR, 12.25 ms; TE, 5.90 ms; NEX, 1;

matrix, 230 × 1024. An 8-channel head coil was used. Patients younger than 5 years were sedated by the anesthesia team.

Twenty-seven patients with enlarged vestibular aqueducts who underwent MR imaging were found in the PACS. Twenty-six of the 27 patients underwent MR imaging for assessment of sensorineural hearing loss. One patient did not have a history of sensorineural hearing loss or an audiogram in the electronic medical record but, rather, was being imaged to assess a possible temporal bone lesion. Thirty-three ears in 28 additional consecutive patients referred by otologists and having undergone MR imaging for unilateral hearing loss, vertigo, or dizziness were used as a healthy control dataset. The asymptomatic, contralateral normal ear in these patients with unilateral hearing loss was used. The healthy control set of patients had audiograms that confirmed normal hearing in the ears used in the dataset.

Reformatted images of the cochlea were created with the MPR tool at the radiologist's viewer (SYNAPSE 3D; Fujifilm Medical Systems, Tokyo, Japan) in a plane parallel to the lateral semicircular canal, a reproducible landmark (Figs 1A and 2A). This plane is perpendicular to the distal limb of the first and second turns of the cochlea. Two observers (K.L.R. and A.F.J.) independently measured the perpendicular distance from the osseous spiral lamina–basilar membrane complex in the upper basal turn (closest to the middle ear) to the point at which the first linear signal void distal (anterior) to the osseous spiral lamina–basilar membrane complex contacts the lateral cochlear wall on magnified images.

For the purpose of this study, this is referred to as distance X. In healthy patients, the distal signal void is the interscalar septum; in patients with abnormal findings, it is presumed to be the dysplastic osseous spiral lamina–basilar membrane neural complex. Examples of these measurements are provided (Figs 1B, -C, and 2B, -C). When available, CT images in a reformatted plane parallel to the lateral semicircular canal were reviewed in the setting of discordant findings.

Statistical analysis was performed with GraphPad Prism software (GraphPad Software, San Diego, California). *P* values were calculated with an unpaired *t* test to compare the mean and SDs between patients with prospectively diagnosed cochlear anomalies and normal-hearing ears. The κ interobserver score was calculated on the basis of the observed agreements regarding whether a cochlea was abnormal or normal.

RESULTS

The 33 normal-hearing ears in 28 patients were studied (mean age, 16.7 years; range, 6 months to 32 years; Table). Patients with normal hearing had distance X measurements ranging from 0.8 to 1.1 mm and a mean distance X measurement of 0.93 ± 0.075 mm. With these patients as a normal reference, a cutoff of 1.2 mm was used to define the lower limit of abnormal because this was >3 SDs (greater than the 99.7th percentile) above the mean of healthy patients.

The 27 patients with enlarged vestibular aqueducts had a mean age of 24.9 years (range, 5 months to 65 years; Table). Prospectively, 17 of the 27 patients (63%) were diagnosed with EVA and

IP-II anomalies. These patients were diagnosed prospectively on the basis of the classic imaging qualitative morphologic abnormalities seen in IP-II primarily on CT, but also applied to MR imaging, including the presence of a flattened interscalar ridge (anchor point) between the upper basal and upper middle turns and the cystlike undersegmented appearance of the cochlea.^{1,6} The mean distance X measurement when there was a cochlear abnormality identified prospectively was 1.55 ± 0.25 mm (range, 1–2.1 mm). One patient who was thought to have a bilateral IP-II anomaly prospectively had a distance X measurement of <1.2 mm in 1 ear, which was included in this cohort. The mean distance X measurement among these patients with cochlear malformations was statistically different from that of patients with normal hearing, $P < .001$. Figure 3 demonstrates the mean distance X measurements, along with the range of values within 2 SDs above and below the mean, in patients with prospectively diagnosed IP-II anomalies and those with normal-hearing ears.

Ten of the 27 patients with enlarged vestibular aqueducts were not prospectively diagnosed with IP-II anomalies; however, 4 of these 10 had abnormal distance X measurements of ≥ 1.2 mm. Therefore, 4/21 (19%) patients found to have abnormal cochleas were identified retrospectively. Three of these 4 patients also underwent CT. In 1 patient, expected flattening of the interscalar ridge (anchor point) between the upper basal and upper middle turns was not seen; however, the modiolus of the abnormal cochlea appeared deficient. The other 2 patients had subtle findings of flattening of the interscalar ridge (anchor point), a deficient modiolus, and absence of the lateral interscalar septum. Figure 4A demonstrates the typical CT findings of IP-II from 1 of the 3 patients who subsequently underwent CT. The corresponding MR imaging demonstrates subtle morphologic features and has a widened distance X (Fig 4B).

Interobserver agreement to determine abnormal and normal cochleas based on the 1.2-mm cutoff was good with a calculated κ score of 0.715.

Patient demographics

	Normal-Hearing Ears	Patients with EVA
Total No. of patients	28 (33 ears studied)	27 (54 ears studied)
Mean patient age (yr)	16.7	24.9
SD of patient age (yr)	11.0	21.5
<i>P</i> value		.08

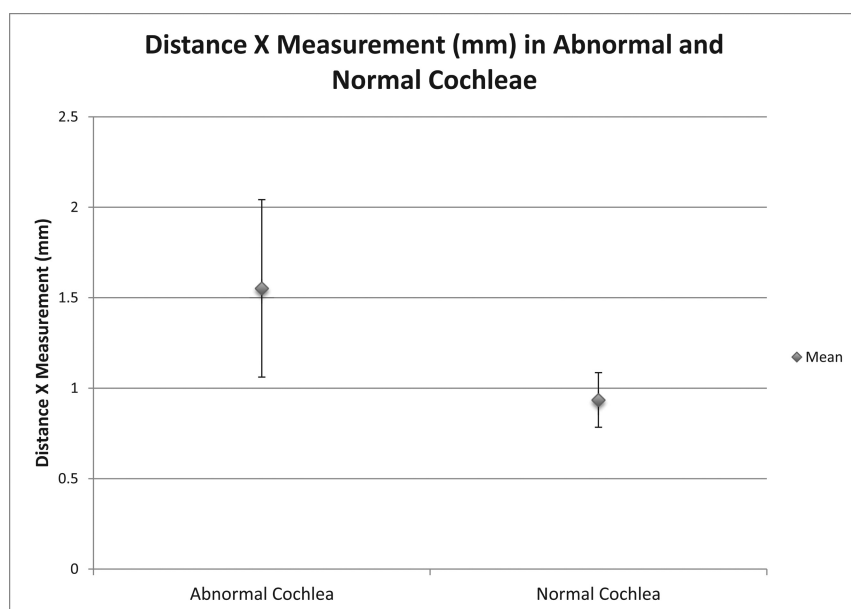


FIG 3. Graph demonstrating the mean distance X measurements \pm 2 SDs in patients with prospectively diagnosed IP-II anomalies and individuals with normal hearing.

DISCUSSION

In patients with a congenital cause of sensorineural hearing loss, an IP-II anomaly of the cochlea is one of the most frequently detected imaging findings. Qualitative appearances of the cochlea on CT have been described in IP-II, including a consistent loss of the interscalar septum and flattening of the interscalar ridge (anchor point) between the upper basal and upper middle turns of the cochlea.⁶ This flattened interscalar ridge may be less apparent on MR imaging because assessment of the bony contour is less optimal. Because more pediatric patients are now undergoing MR imaging for assessment of sensorineural hearing loss, scrutiny of the internal segmentation of the cochlea is important to avoid missing a diagnosis of IP-II.

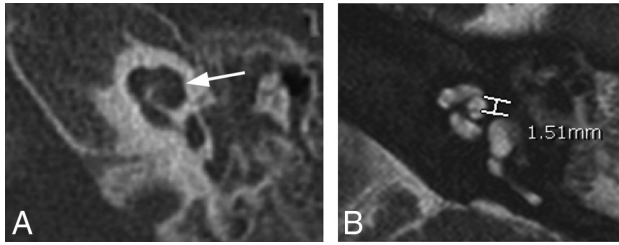


FIG 4. Axial CT and MR images of 1 of the 4 patients who was found, in retrospect, to have abnormal distance X measurements on MR imaging. *A*, On CT, the typical findings of IP-II including flattening of the interscalar ridge (anchor point) between the upper basal and upper middle turns (arrow) are demonstrated and confirm the presence of an IP-II anomaly. *B*, Corresponding MR image, on which distance X is found to be greater than 1.2 mm.

The heavily T2-weighted cisternographic sequence is routinely used in temporal bone imaging and can be performed across MR imaging vendor platforms at both 1.5- and 3T field strengths. On a heavily T2-weighted cisternographic sequence, the basilar membrane of the distal first turn of the cochlea is visible as a hypointense line extending from the modiolus to the lateral wall of the cochlea. Just distal (anterior) to this line, the interscalar septum is normally visible. In IP-II, this segment of the interscalar septum is absent. However, in IP-II, there is a thin T2-hypointense band extending from the lateral modiolus to the lateral wall of the cochlea in the same approximate location, having an appearance similar to that of a slightly malpositioned interscalar septum. On histology, this band corresponds to the dysplastic osseous spiral lamina–basilar membrane neural complex of the second turn and contains neurosensory elements, including a dysplastic organ of Corti on top of a dysplastic basilar membrane.⁴ We hypothesized that a quantitative measurement between the basilar membrane of the upper basal turn of the cochlea and the first T2-hypointense band (distance X) on MR imaging would help differentiate a normal cochlea with an interscalar septum from the IP-II anomaly with the dysplastic osseous spiral lamina–basilar membrane neural complex.

To create a reproducible standardized measurement technique, we identified a plane parallel to the lateral semicircular canal and used axial reconstructions along this plane for measurements. This plane is perpendicular to the distal limb of the first and second turns of the cochlea and can be readily produced at the viewer side with integrated multiplanar reformat tools within most PACS. Distance X measurements in patients with normal hearing had a narrow range from 0.8 to 1.1 mm between the basilar membrane of the upper basal turn and the first low T2 signal band. In the healthy patient, this band represents the anterolateral interscalar septum. The mean distance X measurement was 0.94 ± 0.075 mm. Of note, none of the patients with normal hearing had a distance X measurement exceeding 1.1 mm. Despite the large range in patient age of the normal-hearing ears, the distance X measurement stayed within a relatively small size range, consistent with the development of the cochlea being complete in the embryologic stage.⁷ Distance X measurements in individuals with normal hearing were statistically different from those in patients believed to have IP-II anomalies based on morphologic, qualitative assessment (mean, 1.55 ± 0.25 mm). Prospectively, 1 patient who was thought to have only an EVA on MR imaging and

a suspected bilateral IP-II anomaly prospectively using CT morphology had a distance X measurement of <1.2 mm by both observers (1 and 1.1 mm) in 1 ear. This was considered to be a false-negative, suggesting that measurement criteria should be applied as an adjunct to morphologic criteria. We believe that this false-negative was due to motion degradation on the scan, affecting image quality.

We believed those patients with distance X measurements above 1.2 mm, 3 SDs above the mean, or a measurement greater than the 99.7th percentile to have abnormal cochleas. This method was shown to have good interobserver reliability. With a normal upper limit of 1.2 mm, 78% (21/27) of patients with enlarged vestibular aqueducts had a coexistent cochlear anomaly. This finding was similar to that in other reported studies that have shown EVAs in the presence of cochlear anomalies as high as 76%.⁸ Our study confirms that the EVA has a high association with additional cochlear anomalies.

Retrospective analysis demonstrated that some patients with enlarged vestibular aqueducts might be underdiagnosed with regard to a coexistent cochlear anomaly. Almost one-fifth (4/21) of the patients with EVAs and abnormal cochleas by measurement were found retrospectively. We attribute the presence of a neural band in the lateral cochlea extending to the upper middle turn as a potential reason for the underdiagnosis because the dysplastic osseous spiral lamina–basilar membrane neural complex may be mistaken for a slightly malpositioned or even normally located interscalar septum, thus making this diagnosis more challenging.

Limitations

The major limitation of this study is that only patients with enlarged vestibular aqueducts were assessed. While EVA is commonly associated with cochleovestibular anomalies, cochleovestibular anomalies can also be isolated findings, and these were not assessed. Because a secondary aim of this study was to find underdiagnosed cochlear anomalies, searching our data base for cochlear anomalies alone would be insufficient. Because coexistent cochlear anomalies have been reported in as many as 76% of EVA anomalies,⁸ we decided to focus our attention on this subgroup of patients with hearing loss.

Another limitation of this study is the relatively small sample size. The number of patients with enlarged vestibular aqueducts on MR imaging was relatively rare in our study population. Most of our cases of EVA had been discovered on CT with no further MR imaging performed. Further studies with larger sample sizes may be helpful to confirm our findings.

Theoretically, severe endolymphatic hydrops can displace the osseous spiral lamina–basilar membrane complex toward the scala tympani. However, this phenomenon has only been recognized in the apical turn in severe cases of endolymphatic hydrops in human temporal bone specimens and has not been described in the basal turn.⁹

CONCLUSIONS

The IP-II anomaly is a subtle MR imaging finding. In IP-II, a band of tissue, which histologically represents a combination of dysplastic neural tissue, basilar membrane, and the osseous spiral

lamina, can have an appearance similar to that of an interscalar septum on heavily T2-weighted cisternographic sequences. With a standardized plane parallel to the lateral semicircular canal, a measurement from the basilar membrane of the upper basal turn of the cochlea (closest to the middle ear) to the first T2-hypointense band (distance X) of >1.2 mm should be considered abnormal. Knowledge of the presence of the dysplastic osseous spiral membrane–basilar membrane neural complex and use of a quantitative measurement may help to prospectively reduce missed cochlear anomalies, particularly with an enlarged vestibular aqueduct.

Disclosures: Hugh D. Curtin—UNRELATED: Royalties: Elsevier, Comments: royalties for textbook.

REFERENCES

1. Sennaroglu L, Saatci I. **A new classification for cochleovestibular malformations.** *Laryngoscope* 2002;112:2230–41 CrossRef Medline
2. Sennaroglu L, Saatci I. **Unpartitioned versus incompletely partitioned cochleae: radiologic differentiation.** *Otol Neurotol* 2004;25:520–29; discussion 529 Medline
3. Mondini C. **Minor works of Carlo Mondini: the anatomical section of a boy born deaf.** *Am J Otol* 1997;18:288–93 CrossRef Medline
4. Leung KJ, Quesnel AM, Juliano AF, et al. **Correlation of CT, MR, and histopathology in incomplete partition-II cochlear anomaly.** *Otol Neurotol* 2016;37:434–37 CrossRef Medline
5. Kontorinis G, Goetz F, Giourgias A, et al. **Radiological diagnosis of incomplete partition type I versus type II: significance for cochlear implantation.** *Eur Radiol* 2012;22:525–32 CrossRef Medline
6. Makary C, Shin J, Caruso P, et al. **A histological study of scala communis with radiological implications.** *Audiol Neurootol* 2010;15:383–93 CrossRef Medline
7. Bast T, Anson B. *The Temporal Bone and the Ear.* Springfield: Charles C Thomas; 1949
8. Davidson HC, Harnsberger HR, Lemmerling MM, et al. **MR evaluation of vestibulocochlear anomalies associated with large endolymphatic duct and sac.** *AJNR Am J Neuroradiol* 1999;20:1435–41 Medline
9. Nadol J. **Disorders of unknown or multiple causes.** In: Merchant S, Nadol J, Schuknecht HF, eds. *Schuknecht's Pathology of the Ear.* 3rd ed. Shelton, Connecticut: People's Medical Publishing House; 2010:571–627